Enhancement of photon intensity in forced coupled quantum wells inside a semiconductor microcavity

Hichem Eleuch[1,2], Awadhesh Prasad[1,3] and Ingrid Rotter[1]
[1] *Max Planck Institute for the Physics of Complex Systems, Nöthnitzer Str. 38, D-01187 Dresden, Germany*
[2] *Universite de Montreal, C.P. 6128, Succ. Centre—Ville, Montreal (QC), H3C 3J7 Canada*
[3] *Department of Physics and Astrophysics, University of Delhi, Delhi 110007, India*

We study numerically the photon emission from a semiconductor microcavity containing $N \geq 2$ quantum wells under the influence of a periodic external forcing. The emission is determined by the interplay between external forcing and internal interaction between the wells. While the external forcing synchronizes the periodic motion, the internal interaction destroys it. The nonlinear term of the Hamiltonian supports the synchronization. The numerical results show a jump of the photon intensity to very large values at a certain critical value of the external forcing when the number of quantum wells is not too large. We discuss the dynamics of the system across this transition.

PACS numbers: 71.35.Gg, 05.45.-a, 05.45.Pq, 05.45.Ac

I. INTRODUCTION

Over the past five decades nonlinear equations have been used extensively for a detailed investigation of the optical properties of semiconductors [1–6] because of their potential application in opto-electronic devices [7–9]. In semiconductor nanostructures like quantum wells and quantum dots [10, 11] the coupling between light and matter is enhanced. By this, it may produce more pronounced nonlinear and quantum effects such as a modification of the quantum statistical properties of the emitted light as well as bistability and multistability. These effects were theoretically predicted and experimentally observed by several groups [12–21].

In natural systems as well as in experimental realizations of artificial systems, the presence of an external forcing is unavoidable. An external forcing could be either noise (from the surrounding or inherent within the experiment) or caused by a deterministic perturbation. Sometimes, the external forcing is useful for practical applications but sometimes it entails some degradation of the desired system behavior. Examples of important and useful results obtained by means of external perturbation are stochastic resonances [22, 23], chaos control [24, 25], strange nonchaotic dynamics [26–28] etc. One aspect to explore the nonlinear behavior is to scan the parameters space and to observe how the dynamical complexity depends on the parameters [29–32].

The interaction between nonlinear systems gives rise to new phenomena such as synchronization, hysteresis, phase locking, phase shifting, phase-flip, riddling, amplitude death etc. [33–40]. Recently the coupled nonlinear dynamical systems have been extensively studied from both the theoretical and experimental points of view in a variety of contexts in the physical, biological, and social sciences etc. [33, 34].

In our previous work [41] we explored the dynamics of the field intensities in the high excitation regime inside a semiconductor microcavity containing one quantum well. We observed periodic-doubling, quasiperiodic and direct route to chaos as the forcing strength is changed. These results show various types of dynamics depending on the forcing strength. Furthermore we observed also coexisting periodic and chaotic attractors with riddled basin.

In the present paper we consider a network of quantum wells as shown schematically in Fig. 1: N quantum wells are inside a semiconductor microcavity (schematically represented by two Bragg mirrors M) in the presence of an external forcing. The aim is to analyze the dynamical behavior of the intra-cavity photonic intensity and the intensity of the fluorescent light in the presence of periodic signals. We observed a jump in the intensities of photon and exciton emission at appropriate values of the forcing strength. The maximum of the photon intensity is obtained for an optimal number of quantum wells which should not be too large. Across this transition we see either periodic or chaotic motion depending upon the exciton resonance frequency of the individual quantum wells.

The paper is organized as follows. In Sec. II, we review the derivation of exciton-phonon interaction in the presence on N quantum wells. This is followed by Sec. III where the results for several quantum wells are considered. The results are discussed and some conclusions are drawn in Sec. IV.

II. MODEL

We consider N quantum wells inside a semiconductor microcavity, see Fig. 1. Each quantum well is localized in a position, which corresponds to the maximum of the electromagnetic field inside the microcavity. This system is similar to the one described in detail in [42]. Neglecting the effects of the spins, the interaction with the phonons

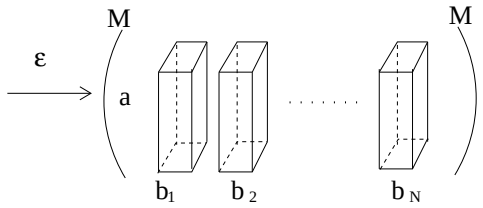

FIG. 1: The schematic model for microcavity with N-quantum wells. Symbols are discussed in text.

and the excitonic saturation, we can write the Hamiltonian describing the system with N quantum wells inside the cavity and pumped with a laser with amplitude ε and frequency ω_L as [43–49]:

$$\begin{aligned} H &= \hbar\omega_{ph}a^{+}a+\sum_{j=1}^{N}\left[\hbar\omega_j b_j^{+}b_j\right]+i\hbar\varepsilon\left(a^{+}e^{-i\omega_L t}-ae^{i\omega_L t}\right) \\ &+\sum_{j=1}^{N}\left[i\hbar g_j^{'}\left(a^{+}b_j-b^{+}a_j\right)+\hbar\alpha_j^{'}b_j^{+}b_j^{+}b_jb_j\right] \end{aligned} \quad (1)$$

The first two terms of the Hamiltonian correspond to the proper energies of photon and quantum well-excitons, where a, b_j are respectively the annihilation operators of a photonic and excitonic modes verifying: $[a,a^{+}]=1$ and $\left[b_j,b_j^{+}\right]=1$. ω_{ph} is the photonic mode frequency and ω_j is the excitonic mode frequency for the j^{th} quantum well. The third term corresponds to the pump energy. The first part of the fourth term represents the exciton-photon coupling with a coupling constant $g_j^{'}$. The last part of the fourth term describes the excitonic nonlinearity for each quantum well with the coefficients $\alpha_j^{'}$.

By considering that the fluctuations are weak compared to the average values, the evolution of the mean field operators in the interaction picture can be written as:

$$\frac{d\langle a\rangle}{d\tau}=\epsilon(t)+\sum_{j=1}^{N}g_j\langle b_j\rangle-\kappa\langle a\rangle-i\Delta_a\langle a\rangle \quad (2a)$$

$$\frac{d\langle b_j\rangle}{d\tau}=-g_j\langle a\rangle-\frac{\gamma_j}{2}\langle b_j\rangle-i\Delta_j\langle b_j\rangle-2i\alpha_j\left\langle b_j^{+}\right\rangle\langle b_j\rangle\langle b_j\rangle \quad (2b)$$

where $j=1,...,N$, τ is a dimensionless time normalized to $\tau_c=\frac{3}{2g_1}$:

$$\tau=\frac{t}{\tau_c}\,, \quad (3)$$

γ_j, κ are the dimensionless decay rates of the excitons and the cavity photon:

$$\gamma_j=\gamma_{ex_j}\ \tau_c;\kappa=\gamma_{ph}\ \tau_c\,, \quad (4)$$

the nonlinear coupling constant α_j and the coupling g_j are normalized to $\frac{1}{\tau_c}$:

$$\begin{aligned} \alpha_j &= \alpha_j^{'}\tau_c \\ g_j &= g_j^{'}\tau_c, \end{aligned} \quad (5)$$

and Δ_a, Δ_j are the dimensionless detuning

$$\begin{aligned} \Delta_a &= (\omega_{ph}-\omega_L)\,\tau_c \\ \Delta_j &= (\omega_j-\omega_L)\,\tau_c. \end{aligned} \quad (6)$$

According to these equations, the coupling among excitonic modes arises from their common interaction with the photonic mode. It represents a global mean field coupling of excitonic modes and is given by the sum term (over j) in (2). Moreover, the evolution of the excitonic modes contains a nonlinear term (last term in (2). It is worth to mention that the nonlinear parameters α_j can be scaled to 1 by redefining $<b_j^{new}>=<b_j>/\sqrt{\alpha_j}$ and $g_j^{new}=g_j*\sqrt{\alpha}_j$. This system has $2(N+1)$-dimensions in the presence of forcing . For the numerical simulation we use RK4 integrator [52]. We consider the step size $\Delta t=2\pi/5000$ for integration. The dynamical studies are studied after removing initial 10^7 data points as transients. We explore here the photon and exciton intensities $I_a=\langle a^{+}\rangle\langle a\rangle$ and $I_j=\left\langle b_j^{+}\right\rangle\langle b_j\rangle$ inside the cavity. As the fluorescent light is proportional to the mean number of excitons (I_j), we are also exploring the fluorescent light dynamics.

III. NUMERICAL RESULTS

The system properties are determined by different physical parameters. In our calculations, we fix some of them in order to have the possibility to determine the influence of the remaining ones. In all our calculations, the normalized parameters are fixed to $g_j=g=1.5$ and $\kappa=0.12$, $\gamma=\gamma_j=0.015$ which correspond to the experimental values [19] in units of the inverse of the round-trip in the microcavity. Furthermore, we concentrate our analysis to the case of a strong pump field where the non-linear phenomena are expected to influence the dynamics. We choose the normalized amplitude of the laser pump as $\epsilon=200$ and the normalized excitonic interaction coefficient as $\alpha_j=\alpha=0.00001$. At this set of parameters the equations describing the dynamics of the system have stable fixed point solutions.

The parameter ϵ characterizes the influence of external forcing on the dynamics of the system. We use it, in the present study, in order to receive information on the effect of the external forcing. We restrict our analysis to a deterministic periodic forcing in ϵ, i.e. $\epsilon\rightarrow\epsilon(1+f\,cos(\Omega t))$ where Ω is the perturbation frequency while f is the strength of the forcing. The last value is considered as bifurcation parameter. As to the first value, we consider only the case $\Omega=1$ in the present work. This value of Ω corresponds to 1.5 Thz physical frequency. The Thz-sources are recently realized [50, 51].

As we change the magnitude of f, various dynamical motions are possible. We have discussed this result recently [41] for the case of one quantum well and different values of the detuning Δ_a and Δ_1. In the present paper we consider the effect of the forcing strength f, of

the detuning Δ_j and of the number N of quantum wells at fixed $\Delta_a = 0$ (the cavity is resonant with the pump laser).

A. Two quantum wells

In order to show the results in details, we first consider two quantum wells. We fix $\Delta_1 = -g$ and vary $\Delta_2 \in [-g, g]$.

Shown in Figs. 2(a,b) are the photon intensities I_a in the parameter space $\Delta_2 - f$, respectively, without ($\alpha_j = 0$) and with ($\alpha_j = 0.00001$) a nonlinear term in the Hamiltonian (1). Fig. 2(a) shows that I_a varies smoothly as a function of the forcing f except near to the value of $\Delta_2 = -0.5$ when the nonlinear term is not considered. The results obtained with inclusion of the nonlinear term show another behavior, Fig. 2(b). Here, the intensity increases smoothly as a function of f for all but a certain critical value of f. At this critical value, I_a jumps to much higher values.

The details of the behavior of I_a are shown in Fig. 3 where the left panel is drawn for fixed $\Delta_1 = \Delta_2 = g$ while the right panel corresponds to $\Delta_1 = -g$ and $\Delta_2 = g$. These two cases correspond to identical and mismatched quantum wells, respectively. The mismatch in the latter case is equal to the Rabi frequency of the single quantum well which is $|\Delta_1 - \Delta_2| = 2g$.

The results shown in Figs. 3(a,b) are obtained with $\alpha_j = 0$, i.e. with a vanishing nonlinear term in the Hamiltonian H, Eq. (1). They show an overall smooth increase of the intensity with increasing forcing strength f. The results in Figs. 3(c,d) are obtained with a nonvanishing nonlinear term in (1), i.e. with $\alpha_j = \alpha = 0.00001$. In this case, I_a does not increase everywhere smoothly with increasing forcing f, see also Fig. 2(b). The nonlinearity causes a substantial jump in the intensity around $f \sim 2$. This jump occurs independently of the detuning Δ_2. In Figs. 3(c,d) the jump is marked by an arrow.

In order to see the dynamical behavior of the system across this transition we plot a few of the largest Lyapunov exponents (LEs) in Figs. 3(e,f) for the nonlinear cases considered in Figs. 3(c) and (d), respectively. The LEs are calculated according to [53]. In the case of identical quantum wells (left panel) the dynamics is always periodic and all but one Lyapunov exponent (which distinguish the type of dynamics, see Ref. [29]) are negative. One of the LEs is zero (dotted line). The third LE (dashed line) is negative but jumps at the same value $f = 1.3$ at which the intensity jumps (shown by an arrow in Fig. 3(c)). The trajectories in the phase space across this transition are shown for two different values of the forcing strength f in Fig. 3(g). The inner black solid line corresponds to $f = 1$ while the outer red-dashed line is for $f = 2$. These results are confirmed by the corresponding Poincaré sections [29] which are taken at $Re\langle a\rangle = 0$, see Fig. 3(i). There are two single points corresponding to $f = 1$ and 2.

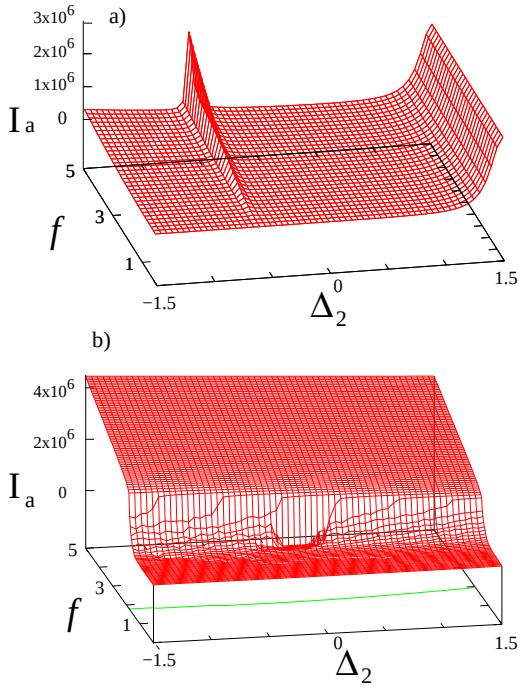

FIG. 2: The photon intensity I_a in the parameter space $\Delta_2 - f$ at the fixed value $\Delta_1 = -g$ for two quantum wells without (a) and with (b) nonlinear term in the Hamiltonian Eq. (1). The contour line in (b) is drawn at $I_a = 2 \times 10^6$.

It should be noted here that both the photon intensity and the exciton intensity jump at the same values of f. The photon intensity is, however, much larger than the exciton intensity, see Fig. 3(c). The variation as a function of time is shown in the insets of Fig. 3(e) which are calculated with the parameters of Fig. 3(g).

In the mismatched case (right panel) we see a behavior of the intensities I as a function of the forcing strength f which is similar to that discussed above for the case with identical wells. Due to the mismatching, the critical values differ from those of the left panel. However the exciton intensities are much smaller than the photon intensities also in this case. The dynamics across the transition is shown in Fig. 3(f). The spectrum of the LEs shows the following characteristic features: below the transition, the motion is chaotic while it is periodic beyond the transition. Both, the chaotic and the periodic motion are shown in Fig. 3(h) with black-solid and red-dashed lines, respectively, at the forcing strengths $f = 1$ and 2. These results are confirmed by the corresponding Poincaré sections taken at $Re\langle a\rangle = 0$ and shown in Fig. 3(j). The motion is chaotic (scattered points) and periodic (single point), respectively. The variation of the intensities as a function of time is shown in the insets of Fig. 3(f) at the parameter values $f = 1$ and 2.

Comparing the results obtained for the case with two identical quantum wells (left panel of Fig. 3) to those obtained with two mismatched wells (right panel of Fig. 3), we state the following. In the first case, the intensities

jump at a certain critical value of the forcing strength f while the transition starts much below this critical value of f in the second case. Note that the y-axis is taken on logarithmic scale. Further, there is a synchronized periodic motion (where the I_j have identical values [33]) across the jump in the first case with identical wells while the motion changes from an unsynchronized chaotic to a synchronized periodic one in the second case with mismatched wells. In any case, the intensities I at large f are much larger when the excitonic nonlinearity in the Hamiltonian Eq. (1) is taken into account, than without this term. The nonlinearity causes, obviously, the jump-like transition to the higher intensities at the critical value of the forcing strength f.

B. Chain of N quantum wells

In order to see the effect of the nonlinearity on the photon and exciton intensities in the case of a large number N of quantum wells we consider in the following a chain of identical quantum wells with fixed $\Delta_j = g$, $\forall j$. In Fig. 4 the calculated photon intensity I_a is drawn in the parameter space : number N of quantum wells and forcing strength f.

According to Fig. 4(a) the intensity I_a decreases smoothly with increasing N (> 2) when the nonlinear term in (1) in not taken into account (corresponding to $\alpha_j = 0$). However there is a jump in intensity from $N = 1$ to $N = 2$. Fig. 4(b) shows the results obtained with inclusion of the nonlinear term in (1), i.e. with $\alpha_j \neq 0$. In this case, the intensity increases first with increasing N and then jumps to lower values. This behavior repeats several times. Both figures indicate further that, at very low forcing strength $f \sim 0$, I_a does not change for any value of N. As a result, a jump in the intensity I_a appears only when the forcing strength f as well as the nonlinearity α do not vanish.

When the nonlinearity in (1) is taken into account in the calculations, a substantial drop in the intensity I_a appears at some values of the forcing strength f when we increase the number N of quantum wells. This behavior of I_a is determined obviously by the nonlinear term in (1). The details of the variation of the photon intensity I_a as well as of the exciton intensity I_j (all I_j are synchronized) are shown in Fig. 5.

Figs. 5(a, b) show numerical results obtained without the nonlinearity in (1) as a function of N and f, respectively. Here, the intensities vary smoothly : the photon intensity I_a as well as the exciton intensity I_j decrease with increasing N but increase with increasing f. The situation is, however, completely different when the nonlinearity is taken into account. In this case, substantial jumps appear in the intensities, see Figs. 5(c,d) and the further results shown in Figs. 5(e-h).

Let us first consider the variation of I_a as a function of N for fixed forcing strength $f = 15$. According to Fig. 5(c), I_a increases first with the number N of quantum wells. However, it reaches a maximum value at $N = 6$ where it decreases suddenly and drops to very low values (even lower than in the single quantum well). The details of the dynamics across this transition are shown in Fig. 5(e). Here, trajectories at $N = 4$ (outer red-dashed line) and 8 (inner black-solid line) are drawn in the phase space $Re\langle a\rangle - Im\langle a\rangle$. These trajectories show periodic motions what is confirmed by the Poincare section shown in Fig. 5(g) with points corresponding to $N = 4$ and 8.

Fig. 5(d) shows the intensity I_a as a function of the forcing strength f for a fixed number $N = 6$ of quantum wells. Similar to the case with two identical wells (Fig. 3(c)) the intensity I_a increases smoothly up to a certain

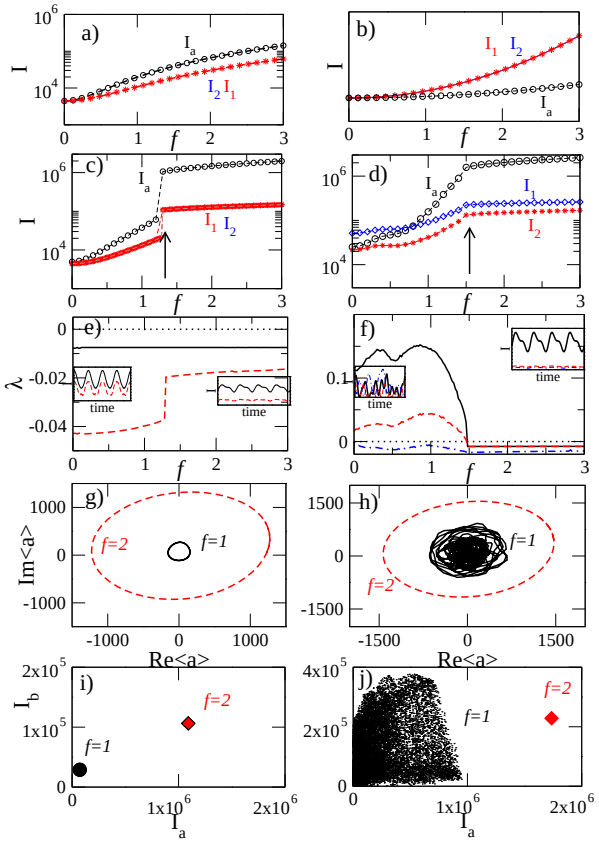

FIG. 3: (Color online) Comparison of some results for two identical quantum wells with those for two mismatched wells. The left and right panels correspond to $\Delta_1 = \Delta_2 = g$ and $\Delta_1 = -g, \Delta_2 = g$, respectively. (a-d): Intensities I_a ($\circ$), I_1 ($\diamond$), and I_2 ($\star$) as a function of the forcing strength f without (a,b) and with (c,d) nonlinear term in (1). The synchronized intensities I_1 ($\diamond$) and I_2 ($\star$) in (a) and (c) are overlapping. (e,f): A few largest Lyapunov exponents as a function of the forcing strength f. The dotted lines represent the zero Lyapunov exponent. Insets in (e,f): intensities I_a (black-solid line), I_1 (red-dashed line) and I_2 (blue-long-dashed line) as a function of time corresponding to (g,h). (g,h): Trajectories in the phase space $Im\langle a\rangle - Re\langle a\rangle$ at $f = 1$ (inner solid line) and $f = 2$ (outer red-dashed line) below and above, respectively, the transition. (i,j): The Poincare section of (g,h). The other parameters are the same as those in Fig. 2.

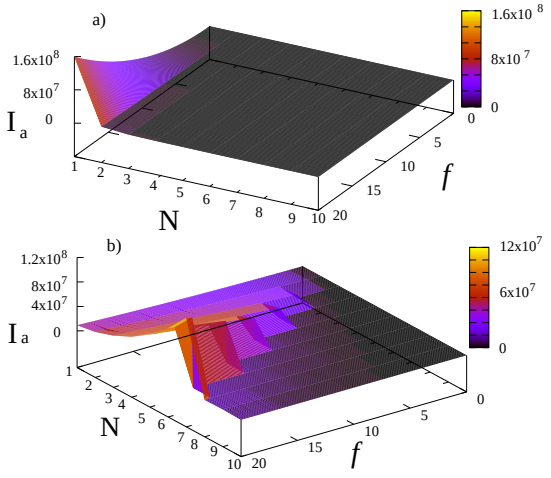

FIG. 4: (Color online) The photon intensity I_a in the parameter space $f - N$ for N identical quantum wells at fixed $\Delta_j = g$, $\forall j$ without (a) and with (b) nonlinear term in (1).

value of f (marked by an arrow in the figure) where it jumps to a much larger value. The corresponding dynamics in phase space $Re\langle a\rangle - Im\langle a\rangle$ is shown in Fig. 5(f) for $f = 10$ (inner black solid line) and $f = 20$ (outer red-dashed line). Both motions are periodic. This result is confirmed by the Poincare section, see Fig. 5(h) where the two corresponding points $f = 10$ and 20 are shown.

The exciton intensities I_j show a similar behavior as the photon intensity I_a in all cases. They are however smaller than I_a.

The results shown in Fig. 5 indicate that the dynamics of the system consisting of N forced coupled semiconductor microwave cavities is determined by two opposite tendencies. On the one hand, the interaction between the quantum wells prevents a synchronized periodic motion. On the other hand, however, the nonlinear terms in the Hamiltonian (1) support the synchronized motion. As a result of these two tendencies, it is possible to increase the photon intensity I_a substantially when the number of quantum wells is not too large.

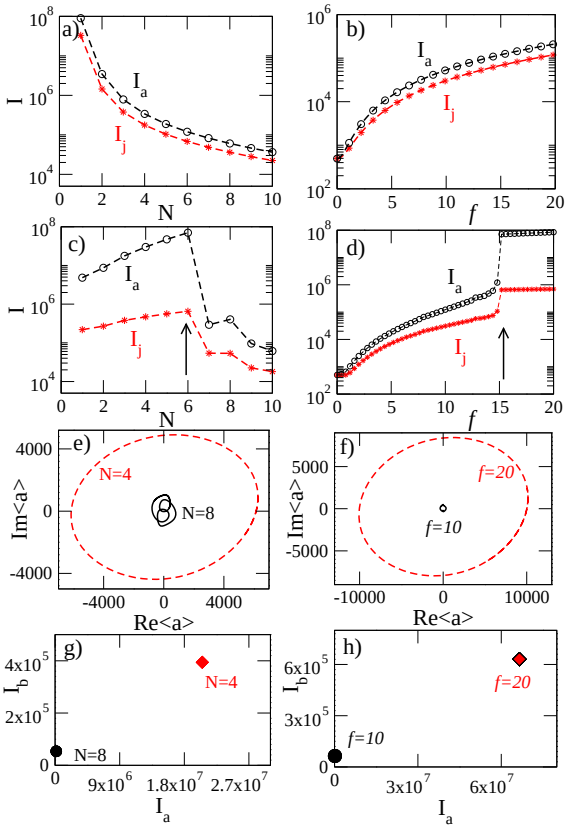

FIG. 5: (Color online) Some results for N identical quantum wells as a function of the number N (at fixed f, left panel) and of the forcing strength f (at fixed N, right panel). (a-d): Intensities I_a ($\circ$) and I_j ($\star$) as a function of N at fixed forcing strength $f = 15$ (a,c) and as a function of f at fixed number $N = 6$ of quantum wells (b,d). The results are obtained, respectively, without (a,b) and with (c,d) nonlinear term in (1). (e,f): Trajectories in phase space $Im\langle a\rangle - Re\langle a\rangle$ at (e) $N = 4$ (outer red-dashed line) and $N = 8$ (inner black solid line) for fixed $f = 15$; and at (f) $f = 10$ (inner solid line) and $f = 20$ (outer red-dashed line) for fixed $N = 6$. (g,h) The Poincare section of (e,f). The other parameters are the same as those in Fig. 4.

IV. DISCUSSION AND CONCLUSIONS

In Sect. III, we showed the calculated intensities of photon and exciton emission from a semiconductor microcavity containing of N quantum wells under the influence of an external forcing f. The intensity of the photon and exciton emission, I_a and I_j respectively, is determined by the interplay of external forcing and internal interaction between the single quantum wells of the microcavity. External forcing synchronizes the periodic motions and causes, by this means, an enhancement of the intensities. The internal interaction, however, disturbs the synchronized motion and leads to a reduction of the intensities of photon as well of exciton emission. The interplay between external and internal interaction is described well by the Hamiltonian (1).

In the case of $N = 2$, the destructive role of the internal interaction is small. The intensities I_a and I_j increase with f starting at a certain small value of f. This holds true for the case of two identical wells as well as for two mismatched wells. In both cases, the intensities jump to much higher values at a certain critical value of the forcing strength f. In the first case, the dynamics of the system is a synchronized periodic motion below as well as beyond the jump. In the second case, however, the motion is unsynchronized chaotic below the critical value of f where the jump occurs, and changes to a synchronized periodic motion for f values beyond the jump.

In the case with N wells, the destructive role of the internal interaction between the wells can directly be seen. Without the nonlinear term in the Hamiltonian (1), the

intensities decrease with increasing N (and fixed f) but increase with f (and fixed N), see Figs. 5(a,b). With nonlinear term in (1), however, the intensities increase first smoothly up to a certain critical value of N (and fixed f), and a critical value of f (and fixed N), respectively, see Figs. 5(c,d). Beyond these values, the intensities decrease abrupt in the first case (Fig. 5(c)) while they jump to higher values in the second case (Fig. 5(d)). In both cases, the intensity I_a jumps by several orders of magnitude at the critical points.

These results illustrate very nicely the interplay of internal interaction between the wells and external forcing. The jump in the intensities is a coherent effect that does not occur in a single quantum well, see the results obtained earlier [41]. The jump in the intensities with a fixed (not too large number N of wells) at a critical value of f is similar to that observed in the case with two wells. In any case, the dynamics across the jump depends on the internal parameters of the quantum wells, and the nonlinear term in the Hamiltonian (1) plays an important role.

The enhancement of the intensity of photons emitted from a microcavity is of great interest for applications. According to the results of the present paper it is possible to manipulate microcavities in such a way that the intensity of emitted light is very large.

H.E. and A.P. thank E. Siminos for valuable comments and acknowledge the financial support and the hospitality of the MPIPKS.

[1] S. Schmitt-Rink, D. A. B. Miller and D. S. Chemla, Phys. Rev. B **35**, 8113 (1997).
[2] G. Khitrova, H. M. Gibbs, F. Jahnke, M. Khira and S. W. Koch, Rev. Mod. Phys. **71**, 1591 (1999).
[3] V. M. Axt and S. Mukamel, Rev. Mod. Phys. **70**, 145 (1989).
[4] C. T. Sah, L. Forbes, L. L. Rosier and Jr. A. F. Tash, Solid-State Electronics **13**, 759 (1970).
[5] E. Garmire and A. Kost, *Nonlinear Optics in Semiconductors I* (Academic Press, London, 1999).
[6] N. Boutabba, L. Hassine, A. Rihani and H. Bouchriha, Synth. Met. **4**, 227 (2003).
[7] T. C. H. Liew, I. A. Shelkhy and G. Mapluech, Physica E **43**, 1543 (2011).
[8] A. Amo, T. C. H. Liew, C. Adrados, R. Houdré, E. Giacobino, A. V. Kavokin and A. Bramati, Nat. Photon. **4**, 361 (2010).
[9] N. Boutabba, L. Hassine, N. Loussaief, F. Kouki and H. Bouchriha, Organic Electronics **4**, 1 (2003).
[10] G. Khitrova, H. M. Gibbs, M. Khira, S. W. Koch and A. Scherer, Nature Phys. **2**, 81 (2006).
[11] T. Yoshie, A. Scherer, J. Hendrickson, G. Khitrova, H. M. Gibbs, G. Rupper, C. Ell, O. B. Shchekin and D. G. Deppe, Nature **432**, 200 (2004).
[12] B. Deveaud, *The Physics of Semiconductor Microcavities* (Wiley-VCH, New York, 2007).
[13] A. Quattropani and P. Schwendimann, Phys. Stat. Sol. B **242**, 2302 (2005).
[14] E. Giacobino, J. P. Karr, A. Baas, G. Messin, M. Romanelli and A. Bramati, Solid Stat. Commun. **134**, 97 (2005).
[15] E. Giacobino, J. P. Karr, G. Messin, H. Eleuch, A. Baas, C. R. Physique **3**, 41 (2002).
[16] G. Messin, J. P. Karr, H. Eleuch, J. M. Courty and E. Giacobino, J. Phys.: Condens. Matter **11**, 6069 (1999).
[17] H. Eleuch, J. M. Courty, G. Messin, C. Fabre and E. Giacobino, J. Opt. B.: Quantum Semiclass.Optics **1**, 1 (1999).
[18] J. P. Karr, A. Baas, R. Houdré, and E. Giacobino, Phys. Rev. A. **69**, 031802 (2004).
[19] A. Baas, J. P. Karr, H. Eleuch, and E. Giacobino, Phys. Rev. A **69**, 023809 (2004).
[20] T. K. Paraso, M. Wouters, Y. Léger, F. Morier-Genoud and B. Deveaud-Plédran, Nature Materials **9**, 655 (2011).
[21] E. A. Cotta and F. M. Matinaga, Phys. Rev. B. **76**, 073308 (2007).
[22] R. Benzi, A. Sutera and A. Vulpiani, J. Phys. A **14**, L453 (1981).
[23] C. Nicolis and G. Nicolis, Scholarpedia, **2(11)**, 1474 (2007).
[24] A. Córdoba, M. C. Lemos, and F. Jiménez-Morales, J. Chem. Phys. **124**, 014707 (2006).
[25] I. Z. Kiss and J. L. Hudson, Phys. Rev. E **64**, 046215 (2001).
[26] C. Grebogi, E. Ott, S. Pelikan and J. A. Yorke, Physica D **13**, 261 (1984).
[27] A. Prasad, S. S. Negi, and R. Ramaswamy, Int. J. Bif. and Chaos **11**, 291 (2001).
[28] A. Prasad, A. Nandi and R. Ramaswamy, Int. J. Bif. and Chaos **17**, 3397 (2007).
[29] M. Tabor, *Chaos and Integrability in Nonlinear Dynamics: An Introduction* (Wiley, New York, 1989).
[30] K. Kaneko, *Collapse of tori and genesis of chaos in dissipative systems* (Wold Scientific Publication, Singapore, 1986).
[31] D. Ruelle and F. Takens, Commun. Math. Phys. **20**, 167 (1971).
[32] H. G. Schuster and W. Just, *Deterministic Chaos: An Introduction* (Wiley-VCH Weinheim, 2005).
[33] A. S. Pikovsky, M. G. Rosenblum, and J. Kurths, *Synchronization: A Universal Concept in Nonlinear Sciences* (Cambridge University Press, Cambridge, U.K., 2001).
[34] K. Kaneko, *Theory and Applications of Coupled Map Lattices* (John Wiley and Sons, New York, 1993).
[35] J. C. Alexander, J. A. Yorke, Z. You, and I. Kan, Int. J. Bif. Chaos **2**, 795 (1992).
[36] A. Prasad, L. D. Iasemidis, S. Sabesan and K. Tsakalis, Pramana, J. Phys. **64**, 513 (2005).
[37] A. Prasad, J. Kurths, S. K. Dana, and R. Ramaswamy, Phys. Rev. E. **74**, 035204 (2006).
[38] A. Prasad, Phys. Rev. E **72**, 056204 (2005).
[39] L. M. Pecora and T. L. Carroll, Phys. Rev. Lett. **64**, 821

(1990).
[40] G. Saxena, A. Prasad and R. Ramaswamy, Physics Reports, (DOI:10.1016/j.physrep.2012.09.003)– in press.
[41] H. Eleuch and A. Prasad, Phys. Lett. **376**, 1970 (2012).
[42] R. Houdre, C. Weisbuch, R. P. Stanley, U. Oesterle and M. Ilegems, Phys. Rev. Lett. **85**, 2793 (2000).
[43] H. Haug, Z. Phys. B. **24**, 351 (1976).
[44] E. Hanamura, J. Phys. Soc. Jpn. **37**, 1545 (1974).
[45] E. Hanamura, J.Phys.Soc.Jpn. **37**, 1553 (1974).
[46] E. A. Sete, H. Eleuch and S. Das, Phys. Rev. A. **84**, 053817 (2011).
[47] H. Eleuch and N. Rachid, Eur. Phys. J. D **57**, 259 (2010).
[48] H. Eleuch, Applied Mathematics & Information Sciences **3**, 185 (2009).
[49] H. Eleuch J. Phys. B: At. Mol. Opt. Phys. **41**, 055502 (2008).
[50] D. Shrekenhamer et al., Optics Express **19**, 9968 (2011).
[51] S. Busch et al., Opt. Lett. **37**, 1391 (2012).
[52] W. H. Press, S. A. Teukolsky, W. T. Vetterling, and B. P. Flannery, *Numerical Recipes: The Art of Scientific Computing* (Cambridge University Press, New York, 1986).
[53] I. Shimada and T. Nagashima, Prog. Theor. Phys. 61 1605 (1979).